IEEE Access
Multidisciplinary ⋮ Rapid Review ⋮ Open Access Journal

Received 31 May 2023, accepted 11 June 2023, date of publication 21 June 2023, date of current version 28 June 2023.

Digital Object Identifier 10.1109/ACCESS.2023.3288281

APPLIED RESEARCH

Directly-Modulated 1310 nm Laser TOSA Developed for Seamless Millimeter Wave Radio Over Fiber Transmission

MATEJ KOMANEC[1], LEOS HALMO[2], VIKTOR ADLER[1], JAN BOHATA[1], MARTA BOTELLA-CAMPOS[3], JAKUB ZVERINA[2], AND STANISLAV ZVANOVEC[1]

[1]Faculty of Electrical Engineering, Czech Technical University in Prague, 166 27 Prague, Czech Republic
[2]Argotech a.s., 541 01 Trutnov, Czech Republic
[3]Department of Communications, Universitat Politècnica de València, 46022 Valencia, Spain

Corresponding author: Matej Komanec (komanmat@fel.cvut.cz)

This work was supported in part by the Project Ministry of Industry and Trade of the Czech Republic TRIO under Grant FV40089, and in part by the Technology Agency of the Czech Republic under Grant FW03010551.

ABSTRACT We present for the first time a directly-modulated high-frequency laser transmitter optical sub-assembly (TOSA) in a commercially-available TO-can packaging working in the 1310 nm band capable of digital transmission at 25 Gb/s and analog transmission up to 25 GHz. We show a step-by-step assembly procedure starting from the TO-can package high-frequency characterization, followed by a bare laser chip analysis and the supporting PCB evaluation to the final TOSA assembly step. We verify the developed TOSA long-term stability by shock and aging tests which had no impact on the TOSA bandwidth or output optical power. We reveal the optimal forward current for digital transmission at 60 mA, and for analog transmission, we operate below the forward current of 40 mA to suppress unwanted laser side modes. We test the TOSA performance by a successful 25 Gb/s on-off keying (OOK) data transmission over a passive optical network with BER of 3.2E-3 and 2.0E-8 for 25 Gb/s, and 10.3 Gb/s, respectively. Finally, we demonstrate analog millimeter wave radio transmission at 25 GHz of a 16-QAM orthogonally frequency division multiplexing (OFDM) signal with 20 MHz bandwidth over a 5 km-long optical fronthaul with a seamless wireless link providing EVM below the 12.5% limit to show real-case scenario performance.

INDEX TERMS Directly-modulated laser, radio-over-fiber, fiber-wireless, 5G networks, microwave photonics.

I. INTRODUCTION

The ever-increasing demand for data rates driven by high-resolution video streaming places significant requirements on ubiquitous broadband signal coverage. Fiber-optic communications are the main enabling technology, where the optical transmitter plays a crucial role in providing the optical signal with modulated data. For modulation, we can use a directly or an externally modulated laser, where the directly-modulated laser (DML) represents the least complex, compact, and low-cost solution [1], [2].

The associate editor coordinating the review of this manuscript and approving it for publication was Prakasam Periasamy.

DMLs in fiber-optic communication are mainly used in the 1550 nm band, where single-mode fibers (SMFs) exhibit the lowest attenuation. On the other hand, the advantage of DMLs use in fiber-optic communication in the 1310 nm band has been as well presented, as this band is appealing especially for applications requiring low chromatic dispersion.

In [1], a DML operating at 1310 nm was used in a digital transmission over very short to medium SMF links. Data rates of 20 Gb/s and 40 Gb/s were achieved for SMF links of 37.5 km and 2.5 km, respectively. A 10 Gb/s DML at a wavelength of 1310 nm was demonstrated in [3] using digital signal processing to experimentally transmit 50 Gb/s for a passive optical network downstream over 20 km-long SMF link. The authors achieved a bandwidth improve-

ment of up to 5 GHz through the interaction of negative chromatic dispersion and the DML chirp. A 100-gigabit Ethernet transmitter optical sub-assembly (TOSA) using a DML array was presented in [4]. This TOSA consisted of four monolithically integrated DMLs in the 1295–1310 nm wavelength range using an optical multiplexer. Here, the authors produced a maximal 3 dB bandwidth per DML of 17 GHz with a possible bit rate of 25.8 Gb/s experimentally demonstrated over 30 km-long SMF link.

Directly modulated DFB lasers at 1310 nm region can be used to serve for high data rate transmission with useable bandwidth exceeding 20 GHz as was shown e.g., in [5]. Authors successfully transmitted 53-Gbaud PAM4 signal over 10 km of SMF using a designed DFB laser at 1300 nm by adopting an asymmetric corrugation pitch modulated grating structure and an InGaAlAs multi-quantum well active layer. In [6], a DFB laser emitting at 1300 nm and using a floating feeding electrode was designed to provide more than 28 mW of optical power with a 3-dB bandwidth of 26 GHz. The proposed laser was capable to transmit up to 45 Gb/s NRZ signals over 35 km of SMF. A DFB laser at 1300 nm wavelength with dual wavelength for THz communications has been presented in [7]. The laser was capable to transmit 25 Gb/s NRZ signal, while the mode tunability enabled frequency separation between 96 and 1510 GHz. Nevertheless, all these demonstrations focused on bare laser chip evaluations only.

Unfortunately, the above-mentioned techniques are relevant only for digital transmission. For analog radio transmission over fiber optics (commonly denoted as radio over fiber (RoF) or radio-frequency over glass (RFoG)) and especially for millimeter wave (mmW) frequency bands, different performance requirements must be fulfilled, such as sufficient laser bandwidth, laser output optical power (to reduce amplification requirements), relative intensity noise (RIN), linearity or laser mode purity (avoiding strong secondary resonances, expressed by the side-mode suppression ratio (SMSR) parameter [8].

In [9], a DML based on the vertical cavity surface emitting laser (VCSEL) and a distributed-feedback (DFB) laser was operated at 1310 nm for an analog RoF transmission at a frequency of 2.14 GHz with a 60 MHz bandwidth. A transmission of 16-quadrature amplitude modulation (QAM) was experimentally tested at 25 km-long SMF link with the error vector magnitude (EVM) below the limit of 12.5% given by the ETSI Technical Specification [10]. The authors highlighted the low-cost solution using a VCSEL instead of a DFB laser for single-mode transmission. An RoF transceiver based on 1310 nm commercial off-the-shelf optical components, *i.e.*, a TOSA using a DFB laser at 1310 nm for 10 Gb/s application, was published in [11] with a 3 dB-bandwidth of 4.3 GHz for the transmission of a 54 Mb/s 64-QAM orthogonal frequency division multiplexing (OFDM) signal.

Two frequency bands of 2.4 GHz and 5 GHz were considered in [12] for low-cost fiber-radio feeding options in pico cellular networks. In addition to the standard wavelength of 850 nm for multimode networks, a directly modulated VCSEL at 1310 nm was also used as a transmitter in the RoF system. Note that the maximal radio carrier frequency was 5.8 GHz while up to 30 km of SMF was deployed. The authors in [13] experimentally demonstrated a new multiband 5G radio-based analog RoF link transmission at 3 GHz and 20 GHz over 15 km of SMF at a wavelength of 1310 nm. However, an external high-frequency Mach-Zehnder modulator (MZM) was used to modulate the analog signal onto the optical carrier.

For emerging high-frequency 5G bands, especially in the frequency range 2 (FR2) (24–28 GHz) [14], low-cost, small-form-factor optical transmitters are still missing. Here, the wavelength band around 1310 nm is extremely attractive for high-frequency analog RoF transmission using intensity-modulated and directly detected (IMDD) systems due to the negligible dispersion-induced fading [15] in standard SMF of arbitrary length and the carrier frequency used.

In this paper, we demonstrate a DML operating in the 1310 nm band in a low-cost, small-form, passive TOSA which can support both high bit rate digital transmission up to 25 Gb/s and analog FR2 radio transmission for up to 25 GHz, which is applicable, for example, in mmW analog radio transmission, in data centers, and for seamless fronthaul scenarios in the framework of 5G networks.

This paper is structured as follows. First, Section II describes laser chip selection and high-frequency TOSA design. Then, TOSA characterization is provided in Section III. Digital and analog signal transmissions over exemplary fiber-optic links are demonstrated in Sections IV, and V, respectively. Section VI then provides the paper's conclusions.

II. TRANSMITTER OPTICAL SUB-ASSEMBLY DESIGN

The first step in our high-frequency TOSA design was laser chip selection. We selected the laser chip primarily based on the capability to transmit digital modulation (25 Gb/s non-return to zero (NRZ)) in situations where the maximal frequency bandwidth was not declared. For 25 Gb/s NRZ, a bandwidth of approx. 18 GHz is typically sufficient (as presented *e.g.*, in [4]). However, for the analog mmW transmission, the demanded bandwidth for mobile networks is at least 24.25 GHz [16]. Such laser chips are commonly packaged into butterfly packages [17] which include an RF port for high-frequency modulation input. However, for packaging into the mmW TOSA, the RF performance of all the TO-can high-frequency circuits and the laser need to fulfill the mmW criterion and this proves to be challenging. These high-frequency aspects of common TO-cans have never been studied, to the best of the authors' knowledge, and this represents one of the key contributions of this paper.

Furthermore, we focused on lasers operating at the 1310 nm band to eliminate dispersion-induced fading critical to analog transmissions. The parameters of the selected high-frequency laser chip, capable of 25 Gb/s digital transmission, are summarized in Table 1.

TABLE 1. Typical parameters of selected laser chips.

Central wavelength	1332 nm
Horizontal full-width at half maximum	27 deg
Vertical full-width at half maximum	38 deg
Maximum output power	11 dBm
Maximum forward current	60 mA
Characteristic impedance	5–10 Ω

The choice of a high-frequency TO-can package was critical, where butterfly packages are commonly used for frequencies above 10 GHz (data rates above 10 Gb/s) [2]. Nevertheless, a TO-can provides two significant advantages compared to the butterfly package: i) a TO-can is cheaper by an order or even more, ii) a TO-can has a simpler construction. On the market, there are numerous TO-cans with various sizes, varying numbers of pins, and characteristic impedance (two common variants are 25 or 50 Ω single-ended and 50 or 100 Ω differentially, respectively). For our TOSA, we have chosen a 50/100 Ω 4-pin TO-can TO-46 package whose preliminary simulations suggested that this TO-can should provide bandwidth over 20 GHz. For this particular TO-can, we then designed and in-house developed a high-frequency micromodule (printed circuit board, PCB), which enabled the 25 GHz operation of the laser chip based on proper impedance matching between the laser chip and the TO-header and overall high-frequency circuitry design.

Next, we measured the microwave properties of the whole TO-can. The TO-header has four pins, out of which two are used for the differential excitation of the laser, which is wire-bonded to the micromodule on the TO-header. These two pins share a common glass dielectric which produces a certain coupling between those pins and influences the microwave properties of the package. The numbering of the microwave ports and their reference planes is shown in Fig. 1a). Input single-ended ports numbered 1 and 2 are placed on the printed circuit board (PCB) where the whole package is soldered. The single-ended ports 3 and 4 are placed on microstrip lines fabricated on a substrate soldered on the top layer of the package (replaced by the micromodule in the next step). In the case of the thru calibration standard connected between ports 3 and 4 (see Fig. 1a)), the reference planes of ports 3 and 4 are merged together.

The direct measurement of the TO-header would be challenging using standard microwave equipment. As we wanted to also include the influence of the package soldering on the micromodule and the wire bonding of the micromodule to the laser, the whole microwave measurement was a two-tier calibration process. First of all, the reference plane of the measurement was transformed on the TO-header to the locations of ports 1 and 2 using the unknown-open-short-match (UOSM) method [18] up to 10 GHz and the multi-line thru-reflect-line (mTRL) method [19] up to 40 GHz. Then, a set of calibration standards on the substrate was embedded and measured on the TO-header. To properly describe the coupling between the pins in a shared dielectric, a 16-term

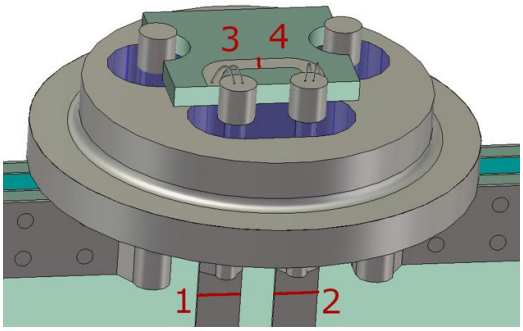

a)

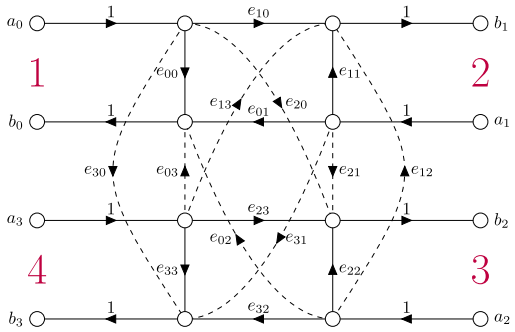

b)

FIGURE 1. TO-header characterization, a) TO-header model with 4 measurement ports and thru calibration standard connected, b) 16-term error model.

calibration model [20] shown in Fig. 1b) was used. The result of the calibration then represents a 4-port error box describing the TO-header. The whole measurement procedure was carried out using a Rohde & Schwarz ZVA67 vector network analyzer (VNA).

To test the reachable operational bandwidth of the TO-header, we carried out a measurement where ports 1 and 2 were differentially excited and an ideal 100 Ω resistor was connected between ports 3 and 4. Thus, ports 1 and 2 formed a logical differential port 1 (see the resulting reflection S_{dd11} in Fig. 2). We can see that the TO-header works well up to ∼28 GHz, where S_{dd11} is over −10 dB (here we do not account for the region around 20 GHz where S_{dd11} is slightly over −10 dB). This result is satisfactory, as expected, for the 25 Gb/s NRZ signal but also for the mmW analog transmission at the FR2 band.

The second step was the laser chip frequency response characterization. We wire-bonded the bare laser chip on a ceramic PCB with a coplanar waveguide (CPW) and fed the laser chip via a probe, as shown in the inset of Fig. 3. The PCB with the CPW had dimensions of 4.6 x 9.0 mm. The reference plane of the measurement was placed on the CPW 1 mm ahead of the laser chip, i.e., the influence of the probe itself was eliminated. The laser was directly modulated with a microwave signal. The output optical signal was captured by a bare SMF, flat-cleaved, and aligned using a 5D micro-

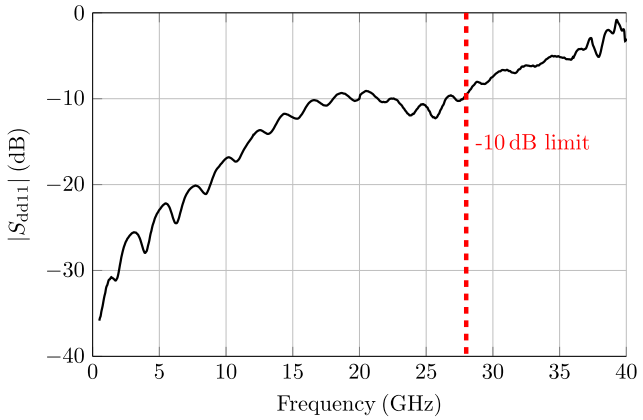

FIGURE 2. Reflection S_{dd11} of the TO-can.

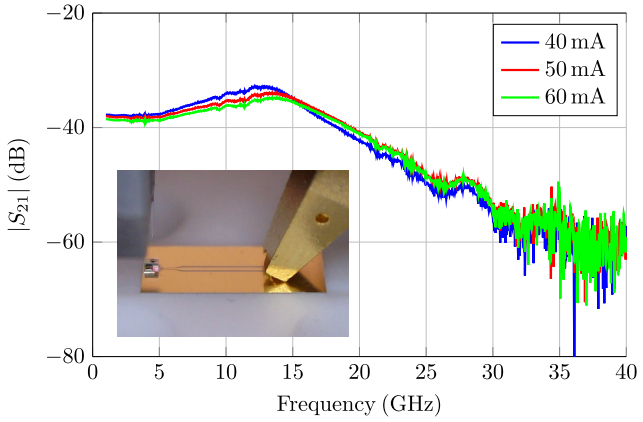

FIGURE 3. $|S_{21}|$ frequency characteristics of the bare laser chip at 40, 50, and 60 mA forward current, inset shows the laser chip excitation using an external probe.

movement stage for maximum optical power. Afterward, the signal was captured by a 40 GHz photodiode (PD, Optilab PD40). We tested three forward current levels to analyze the high-frequency performance of the laser chip. The measured bare laser chip frequency response was corrected by the photodiode's optical-electrical characteristics. The results are shown in Fig. 3. According to the obtained results for 40, 50, and 60 mA, the forward current of 60 mA provides the best frequency response uniformity along with 50 mA. Forward current of 40 mA exhibits a more profound peak at 13 GHz and then drops faster having slightly lower bandwidth than for 50 mA and 60 mA forward currents. As at forward current of 60 mA we obtain the maximal optical output power, we, therefore, used 60 mA as the optimal forward current for the following measurements (apart from the analog signal transmission as discussed later).

We characterized the optical spectra of the bare laser chip at the maximum forward current of 60 mA using a high-resolution optical spectral analyzer (Yokogawa AQ6370) with a maximum resolution of 0.02 nm. The results depicted in Fig. 4 show multiple resonances with the side-mode suppression ratio (SMSR) over 20 dB providing a reasonably

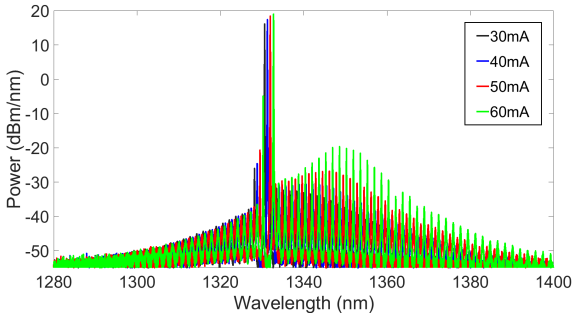

FIGURE 4. Optical spectrum of the bare laser chip at various forward currents.

single-moded regime that is vital in analog signal transmission (as discussed in detail in Section V). We see that the SMSR decreases as the forward current rises, being at 42 dB for both 30 mA and 40 mA, slightly decreasing to 39 dB for 50 mA and finally plummeting to 24 dB at 60 mA. Moreover, at 50 mA and 60 mA, relatively strong peaks at longer wavelengths appear and thus wider the overall optical bandwidth, which might be detrimental for analog signal transmission.

In the third step, we soldered the fully-populated micromodule (high-frequency PCB) onto the TO-header. The micromodule included the wire-bonded laser chip, a 45° mirror placed next to the laser chip, a matching resistor, a bias tee, a monitoring photodiode, and a high-frequency capacitor.

Finally, we covered the TO-header with a cap that had an optical window deposited with an anti-reflective coating for the 1310 nm band. Then we aligned the optical output to a standard single-mode fiber (SMF) with respect to maximum output optical power and attached the SMF to the TO-can resulting in the final TOSA. The output optical power was for all TOSA in the range of 9-10 dBm (at 60 mA forward current), which is advantageous for analog data transmission. It is worth mentioning that the coupling loss from chip to fiber is about 2 dB. Note that an identical process would be carried out for laser chips at the 1550 nm band, with the only modification of a suitable anti-reflective coating at the cap window.

To ensure long-term stability, we carried out temperature shock tests (up to +85°C for 30 mins, then down to 0°C for 30 mins in repeated cycles for 100 h) and aging tests (+85°C and 85% relative humidity for 100 h). We have not seen any change in the TOSA bandwidth nor in the output optical power.

III. HIGH-FREQUENCY TOSA CHARACTERIZATION

To characterize the microwave behavior of the assembled TOSA, a suitable high-frequency driver was first required. Since there was no commercially available solution on market, we proposed our own driver - an evaluation board with a high-frequency amplifier (HMC7810A, Analog Devices). To analyze the bandwidth of the amplifier/evaluation board,

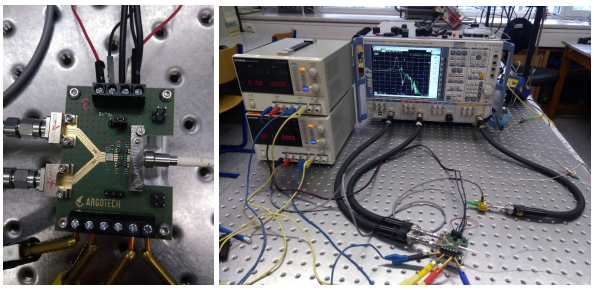

a) b)

FIGURE 5. Measurement setup, a) TOSA connected to the evaluation board, b) VNA connected to the evaluation board and to PD.

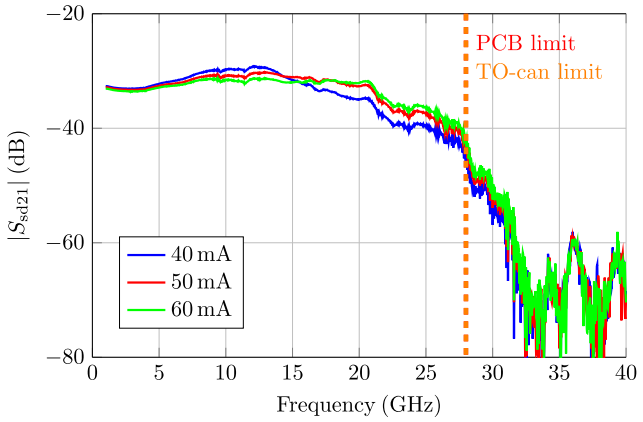

FIGURE 6. Transmission frequency characteristics, $|S_{sd21}|$, of TOSA at 40, 50, and 60 mA forward currents using an in-house built microwave laser driver.

we measured the amplifier characteristics in a differential input and differential output configuration with two pairs of 2.92 mm connectors (End-Launch, Southwest Microwave). We again used our 4-port VNA capable of measuring all mixed-mode *S*-parameters of the amplifier and evaluation board.

We measured differential transmission S_{dd21} up to 40 GHz and verified the amplifier data sheet parameters with a bandwidth of 28 GHz. This bandwidth matches the 28 GHz limit provided by the TO-header itself which means the amplifier does not limit TOSA bandwidth characterization.

Then, we connected our TOSA sample to the evaluation board and characterized the microwave response of the whole TOSA assembly. To do this, we connected a VNA to the input side of the evaluation board with the TOSA and a photodiode (PD, Optilab PD40) at the output side. We monitored the laser output power at a 99/1 coupler with a power meter (PM, Thorlabs PD100 + S122C) and ensured the power level at the PD by adjusting a variable optical attenuator (VOA, OZ Optics DA100). The TOSA was connected to the driver on a PCB, see Fig. 5a). The experimental setup is illustrated in Fig. 5b).

As stated above, we have measured our TOSA samples at forward currents of 40, 50, and 60 mA (as during the laser chip characterization). Fig. 6 shows the resulting frequency characteristics for up to 40 GHz. The S_{sd21} represents the transmission between differential amplifier input and PD single-ended output. Note that the measured data were corrected by using the PD frequency response. It can be seen that our evaluation board limits TOSA performance at around 28 GHz, which is in absolute correlation to the frequency response measured previously, and the limiting frequency of the TO-header is defined by the level of back-reflection, S_{11} (see Fig. 2). The decrease at around 20.5 GHz is attributed to the contribution of the TOSA packaging itself, as such a drop in the frequency spectrum was not observed in any previous measurement of any singular component of the TOSA. Overall, adding the cap to either the TO-header forming the TO-can or the final TOSA assembly does not deteriorate the high-frequency performance.

IV. DIGITAL SIGNAL TRANSMISSION

To analyze the data transmission performance of our TOSA for a real system, we carried out a 25 Gb/s digital signal transmission test. To do this, we used a bit analyzer and an eye analyzer (EXFO BA-4000 and EXFA EA-4000) to generate and analyze the non-return-to-zero (NRZ) on-off-keying (OOK) signal. The generator and analyzer were directly connected by a coaxial cable for mutual clock synchronization. Then, the generator signal output was coupled to the evaluation board with the TOSA using a differential RF input (as used for the frequency characterization described above). The TOSA output optical fiber was connected to the VOA. In the case scenario, a 10 km-long SMF spool was included after the VOA to evaluate the transmission performance for a long fiber link (not shown in Fig. 7). Then the VOA output was connected to a 50/50 coupler, one pigtail leading to the eye analyzer, which has an optical input, and the other pigtail coupled to the 40 GHz PD, thus converting the signal back to the electrical domain to obtain both the eye diagram and bit-error-rate (BER). The electrical signal from the PD was amplified using the same amplifier as the one used in the evaluation board and led back to the input of the bit analyzer for BER analysis. The measurement setup is depicted in Fig. 7.

An OOK NRZ modulation with differential signaling and a symbol rate of 25 GBd was used for the BER analysis while employing PN7 pseudo-random bit sequences. The TOSA operated at 60 mA resulting in an optical output power of 10 dBm.

BER performance was measured for increasing link insertion loss (IL) up to 12 dB, as shown in Fig. 8, which evinces a potential link margin for the deployment of optical components to the link in addition to the 10 km of SMF. Note that the VOA itself has an IL of 1.9 dB. Data show a relatively small difference between the 10.3 Gb/s and 25 Gb/s performance with enough optical power margin, *i.e.*, more than 8 dB, even while the 10 km fiber is used. BER magnitude

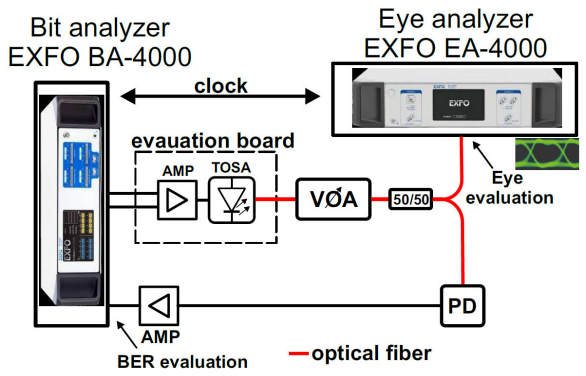

FIGURE 7. Back-to-back configuration for the BER and eye-diagram analysis.

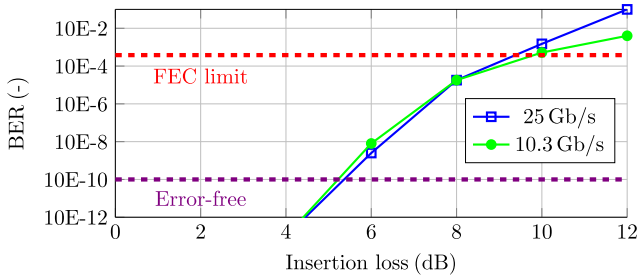

FIGURE 8. BER dependence on additional losses introduced by the VOA for PN7 sequences at 10.3 Gb/s and 25 Gb/s, respectively.

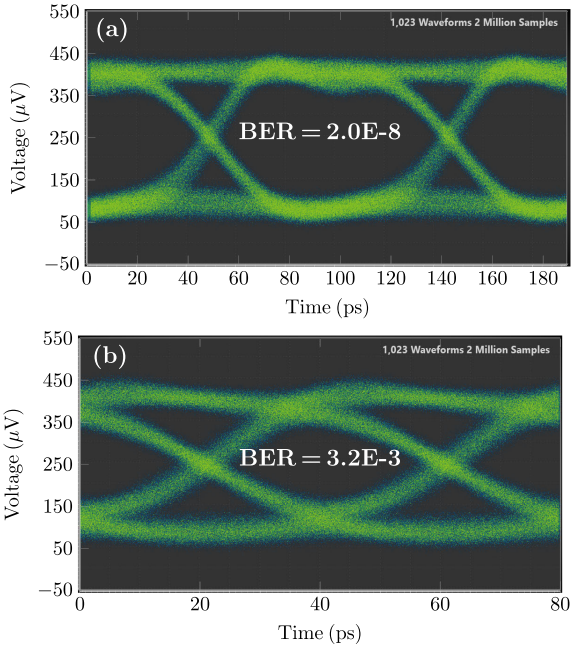

FIGURE 9. Eye diagrams for a) 10.3 Gb/s, and b) 25 Gb/s at the output of the proposed PON.

below 10E-10 is not shown by the equipment used and is considered error-free.

Furthermore, to demonstrate a real high-bit rate application for digital signal transmission, we created a customized passive optical network (PON) testbed consisting of the previously used 10 km-long SMF, with an additional 1:8 power splitter and another 3 km-long SMF emulating the user connection, *i.e.*, the ''last mile''. The total loss of the proposed PON was 15.7 dB while the measured maximum BER with PN7 sequence was 3.2E-3 and 2.0E-8 for 25 Gb/s, and 10.3 Gb/s, respectively. Moreover, the obtained eye diagrams of the signal received after the proposed PON are shown in Figure 9. Therefore, we confirmed the developed TOSA usability to be up to the OOK NRZ 25 Gb/s transmission in an access network. Although the 25 Gb/s transmitting format has been chosen especially because it is widely used and it was the declared bit rate for the chosen chip, we also verified the capability of the developed TOSA to successfully transmit 28 Gb/s OOK NRZ signal with BER of 2.7E-6 (PN31), which was, in fact, the maximal bit rate of the used bit analyzer.

V. ANALOG SIGNAL TRANSMISSION

In microwave photonics, *i.e.*, in RoF, transmission links using IMDD suffer from chromatic dispersion-induced fading [21]. This is due to analog photocurrents generated by each sideband destructively interfering in dual sideband transmission at particular frequencies. This is especially detrimental for long fiber links or high-frequency operation, *i.e.*, approx. for frequencies over 10 GHz. This is true, in particular, for the conventional communication systems operating in the C-band (1525–1565 nm) where the chromatic dispersion coefficient in conventional optical SMFs is around 17 ps/nm·km.

In contrast, our developed TOSA emits at 1332 nm where the chromatic dispersion is significantly lower, *i.e.*, approx. 2 ps/nm·km. Although chromatic-dispersion-induced fading is still present, it can be neglected for frequencies up to 35 GHz when using 10 km of SMF (calculated using Eq. 3 from [22]). Otherwise, when the 1550 nm band is used, a single sideband transmission regime needs to be applied to the fading suppression but at a price of increased complexity of the transmission system.

To verify TOSA usability for mmW transmission towards new generation mobile networks, we prepared a measurement configuration (see Fig. 10) representing a typical RoF fronthaul scenario, which included a vector data signal generator (Rohde & Schwarz, SMW200A) providing the 16-QAM baseband IQ signal with a bandwidth of 20 MHz using long-term evolution (LTE) test model TM 3.2 [10]. A single tone carrier at 25 GHz with RF power of 18 dBm was generated using a signal generator (Rohde & Schwarz SMF100A). The baseband IQ data were up-converted to the desired 25 GHz by using an IQ mixer while the output 20 MHz-bandwidth RF mmW signal at 25 GHz was fed to our TOSA. The TOSA had differential input, so the RF signal was connected to the one input, whereas the second was terminated with the 50 Ω load. The TOSA output optical fiber was connected to a polarization controller (PC),

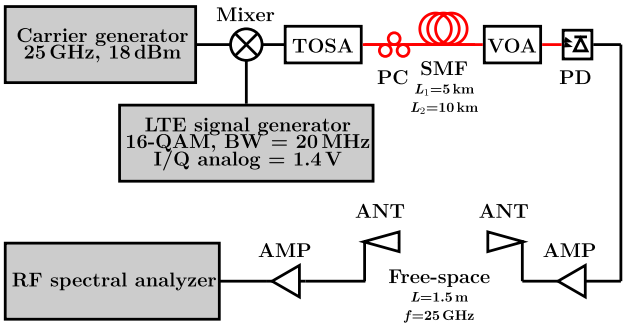

FIGURE 10. The configuration of the mmW analog photonic link measurement.

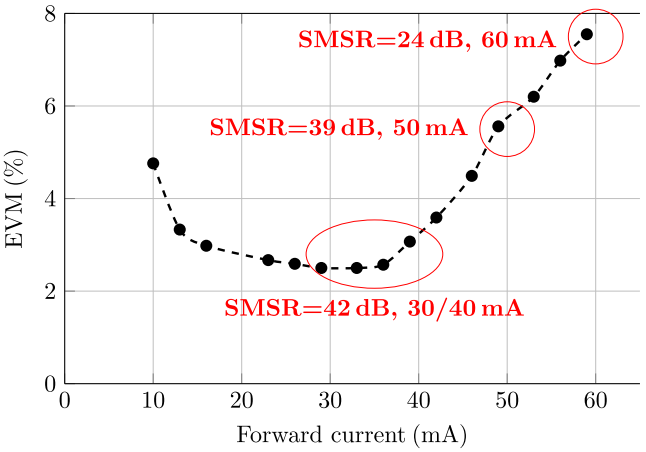

FIGURE 11. Error-vector magnitude (EVM) dependence on the TOSA forward current, SMSR - side-mode suppression ratio at given forward current levels of the laser chip resonance peaks as shown in Fig. 4.

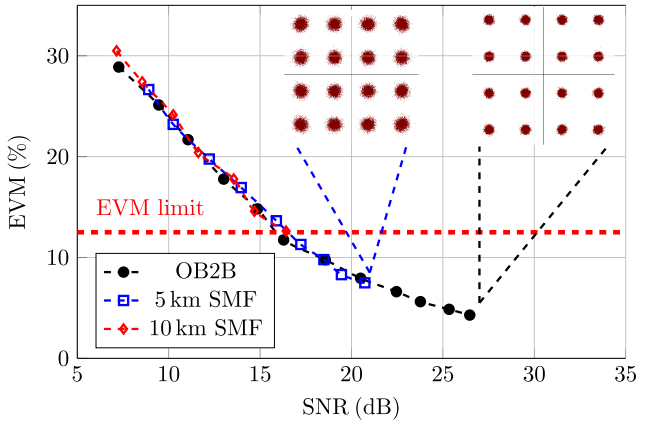

FIGURE 12. A 25 GHz RoF transmission using developed TOSA with 16-QAM modulation for different fiber lengths with an additional 1.5 m-long seamless antenna link.

which ensured polarization insensitivity of the setup, and subsequently to the SMF link of 5 km or 10 km in length. Optical power was then adjusted using the VOA and directly detected by the PD (Optilab PD40). The detected signal was afterward amplified by an RF amplifier (AMP) in the electrical domain and sent to the 1.5 m-long RF antenna link by means of two double ridged horn antennas (ANT, RFSpin DRH40). After the free-space seamless transmission, the received signal was again amplified and finally analyzed with an RF spectral analyzer (Rohde & Schwarz FSW26). It should be noted that the gain of the used amplifier is 24 dB and the noise figure is 4 dB.

The 1.5 m-long antenna seamless link was to emulate a real-case scenario of a remote antenna site connected over the optical analog fronthaul network while using a low-cost optical transmitter in the central office. The short 1.5 m length of the antenna seamless link was given by the laboratory constraints and can be in practice much longer once more RF amplifiers are added.

As our laser exhibited noticeable side resonances in the optical spectrum (see Fig. 4), which depend on the applied current, we first investigated TOSA performance with respect to the forward current. The analysis was carried out in an optical back-to-back (B2B) configuration having the TOSA connected directly to the PD. We focused on the error vector magnitude (EVM) parameter and tuned the forward current from 10 mA up to the maximum current of the laser, *i.e.*, 60 mA, while measuring the side-mode suppression ratio (SMSR). Results of this characterization are shown in Fig. 11. Once we correlate the SMSR values from Fig. 4 with the measured EVM-current dependence, we can identify a region between 15 mA to 40 mA where the TOSA works with reasonably low EVM below 3 %. In this range, the TOSA emits lower optical power (from ∼3 dBm at 15 mA to ∼7 dBm at 40 mA) than with the maximum current of 60 mA (> 10 dBm). For further measurements, we, therefore, operated the TOSA in this current range.

To find the transmission limits, we additionally tuned the VOA from an IL of 0 dB to 12 dB, similar to the PON scenario, to reveal the optical margin and observed the EVM parameter which is dependent on the signal-to-noise ratio (SNR). Results of EVM dependence on the SNR, changed by the variable VOA IL in the optical domain, with the seamless antenna link at 25 GHz for three scenarios are shown in Fig. 12.

It can be seen that all three scenarios, *i.e.*, optical back-to-back (OB2B), 5 km and 10 km of SMF show very similar EVM dependence on the different SNR. Obviously, the OB2B reaches the highest SNR magnitude of all, followed by the 5 km and 10 km SMF scenarios, respectively. However, once considering the EVM limit of 12.5% for the 16-QAM signal, the minimal achieved EVM for the 10 km-long SMF section is slightly over this limit with a value of 12.65 %. Therefore, in order to lower the EVM magnitude, an optical amplifier will be needed to boost the optical signal level in front of the PD, reduce electrical bandwidth or use lower order modulation like quadrature phase-shift keying (QPSK). It should also be emphasized that the system at 25 GHz can operate using 5 km of SMF, which is enough range for most of the fronthaul scenarios, with the received SNR higher

than 21 dB and an EVM of 8% for a 16-QAM modulation scheme with 20 MHz bandwidth without the use of an optical amplifier. Therefore, the proposed TOSA represents a simple and versatile cost-effective solution for RoF systems operating in the mmW frequency range towards the dense deployment of small cells in a 5G network.

VI. CONCLUSION

In this paper, we have presented the development process of a versatile high-frequency TOSA working at 1332 nm and capable of both digital and analog transmission at 25 Gb/s and 25 GHz, respectively. Our developed TOSA presents a low-cost solution implied by using the TO-can assembly, which can be easily mass-produced, compared to the traditional butterfly packaging for high-frequency lasers.

We have first characterized the standalone TO-can package exhibiting satisfactory impedance matching up to 28 GHz considering the −10 dB limit. Then we characterized bare laser chips showing bandwidth up to 21 GHz considering the 3 dB criterion which is sufficient for 25 Gb/s digital transmission needing around 18 GHz bandwidth. Considering analog transmission, the laser chip worked up with lower transmission to almost 30 GHz. Once packaged in the TO-can, resulting in the final TOSA, we verified bandwidth up to 28 GHz limited by our in-house developed PCB/amplifier and the TO-can package.

To ensure long-term stability, we carried out temperature shock tests and aging tests, where we have not seen any change in the TOSA bandwidth nor in the output optical power.

We have studied the optimal conditions for digital and analog transmission using the same TOSA and revealed that the key factor is the forward current level, as for digital transmission performance the maximum forward current, i.e., 60 mA, corresponding to the maximum output optical power is desired. In contrast, for analog transmission performance, the side-mode suppression ratio of the laser has been identified as critical. Therefore, the optimal forward current for analog transmission was in the range of 15–40 mA to obtain suppression of side modes better than 40 dB.

Finally, we demonstrated that our high-frequency TOSA working at 1332 nm performs with BER of 3.2E-3 for 25 Gb/s and 2.0E-8 for 10 Gb/s OOK NRZ data transmission, respectively, for fiber-optic links as long as 10 km in a passive optical network topology. For analog signal transmission, a real-case scenario with 5 km of SMF and a 1.5-long seamless antenna link showed the potential of our TOSA in radio access networks showing EVM below 12.5% at SNR levels over 16 dB. Also, we have demonstrated the 16-QAM transmission over a 10km-long SMF link while the EVM performance was however slightly over the limit for the given signal test model. In order to lower the EVM magnitude, an additional optical amplifier, bandwidth reduction, or different modulation format would be needed.

In comparison with the state-of-the-art results at the 1310nm band [5], [6], [7], we have shown for the first time a high-frequency TOSA using a commercially-available TO-can packaging working up to 25 GHz. Furthermore, we have, for the first time, demonstrated both digital and analog signal transmission using a single TOSA. The bandwidth achieved is comparable to results achieved at the 1310 nm band for bare laser chips [5], [6]. On the other hand, the developed TOSA does not excel, compared to the other published works, in the maximal digital bit rate since the used chips were designed for the 25 Gb/s operation although also successful 28 Gb/s transmission has been presented in this work. Considering output optical powers, the results are at parity with the results presented for bare-chip DMLs in [5] and [7] and just 3 dB lower than in [6]. Such a comparable outcome is excellent considering all the constraints of the TO-can packaging.

This work demonstrates that low-cost, small-form TOSA in the 1310 nm band is a viable solution for any network or system requiring up to 28 GHz bandwidth.

REFERENCES

[1] B. Huiszoon, R. J. W. Jonker, P. K. van Bennekom, G.-D. Khoe, and H. de Waardt, "Cost-effective up to 40 Gb/s transmission performance of 1310 nm directly modulated lasers for short-to medium-range distances," *J. Lightw. Technol.*, vol. 23, no. 3, pp. 1116–1125, Mar. 2005.

[2] J.-H. Song, M. Rensing, C. L. M. Daunt, W. Han, S. Weber, P. A. O'Brien, and F. H. Peters, "High speed laser diode packaging with over 10 GHz-bandwidth," in *Proc. Eur. Conf. Integr. Opt. (ECIO)*, 2010, pp. 1–2.

[3] L. Xue, L. Yi, W. Hu, R. Lin, and J. Chen, "Optics-simplified DSP for 50 Gb/s PON downstream transmission using 10 Gb/s optical devices," *J. Lightw. Technol.*, vol. 38, no. 3, pp. 583–589, Feb. 1, 2020.

[4] S. Kanazawa, W. Kobayashi, Y. Ueda, T. Fujisawa, K. Takahata, T. Ohno, T. Yoshimatsu, H. Ishii, and H. Sanjoh, "30-km error-free transmission of directly modulated DFB laser array transmitter optical sub-assembly for 100-Gb application," *J. Lightw. Technol.*, vol. 34, no. 15, pp. 3646–3652, Aug. 1, 2016.

[5] N. Sasada, T. Nakajima, Y. Sekino, A. Nakanishi, M. Mukaikubo, M. Ebisu, M. Mitaki, S. Hayakawa, and K. Naoe, "Wide-temperature-range (25–80 °C) 53-gbaud PAM4 (106-Gb/s) operation of 1.3-μm directly modulated DFB lasers for 10-km transmission," *J. Lightw. Technol.*, vol. 37, no. 7, pp. 1686–1689, Apr. 1, 2019.

[6] R.-Y. Chen, Y.-J. Chen, C.-L. Chen, C.-C. Wei, W. Lin, and Y.-J. Chiu, "High-power long-waveguide 1300-nm directly modulated DFB laser for 45-Gb/s NRZ and 50-Gb/s PAM4," *IEEE Photon. Technol. Lett.*, vol. 30, no. 24, pp. 2091–2094, Dec. 15, 2018.

[7] Q. Tang, Y. Liu, L. Zhang, X. La, S. Liang, L. Zhao, and W. Wang, "25 Gb/s directly modulated widely tunable 1.3 μm dual wavelength DFB laser for THz communication," *IEEE Photon. Technol. Lett.*, vol. 32, no. 7, pp. 410–413, Apr. 1, 2020.

[8] V. J. Urick, K. J. Williams, and J. D. McKinney, *Fundamentals of Microwave Photonics*. Hoboken, NJ, USA: Wiley, 2015.

[9] R. Alemany, J. Perez, and R. Llorente, "UMTS radio-over-fiber pico-cell interconnection employing uncooled DFB lasers for multi-mode fibre modulation bandwidth enhancement," in *Proc. IEEE LEOS Annu. Meeting Conf.*, Nov. 2009, pp. 699–700.

[10] *ETSI Technical Specification 3GPP TS 136.141 Version 12.6.0 Release 12: LTE; Evolved Universal Terrestrial Radio Access; Base Station Conformance Testing*, document TS 36.141, Version 12.6.0, Release 12, ETSI Technical Specification, 3GPP, Feb. 2015.

[11] Z. Tang, K. Xu, Y. Pei, C. Hua, X. Song, M. Chen, Y. Ji, and J. Lin, "A cost-effective broadband RoF transceiver based on COTS GbE optical components," in *Proc. IEEE Int. Topical Meeting Microw. Photon.*, Sep. 2012, Pp. 148–151.

[12] M. Sauer, A. Kobyakov, and J. George, "Radio over fiber for picocellular network architectures," *J. Lightw. Technol.*, vol. 25, no. 11, pp. 3301–3320, Dec. 6, 2007.

[13] M. U. Hadi, M. Awais, M. Raza, and S. Kausar, "Performance enhancement in multiband 5G NR-radio-over-fiber system using DPD," in *Proc. Int. Topical Meeting Microw. Photon. (MWP)*, Nov. 2021, pp. 1–4.

[14] *3rd Generation Partnership Project; Technical Specification Group Radio Access Network; NR; User Equipment (UE) Radio Transmission and Reception; Part 2: Range 2 Standalone (Release 17)*, document (TS) 38.101-2, Version 17.7.0, 3rd Generation Partnership Project (3GPP), Technical Specification, Sep. 2022.
[15] C. Lim, A. Nirmalathas, M. Bakaul, K.-L. Lee, D. Novak, and R. Waterhouse, "Mitigation strategy for transmission impairments in millimeter-wave radio-over-fiber networks [invited]," *J. Opt. Netw.*, vol. 8, no. 2, pp. 201–214, Feb. 2009.
[16] *5G; NR; Base Station (BS) Conformance Testing Part 2: Radiated Conformance Testing (3GPP TS 38.141-2 Version 15.8.0 Release 15)*, document 138 141-2, Version 15.8.0, 3rd Generation Partnership Project (3GPP), Technical Specification (TS), Sep. 2022.
[17] J. Kreissl, V. Vercesi, U. Troppenz, T. Gaertner, W. Wenisch, and M. Schell, "Up to 40 Gb/s directly modulated laser operating at low driving current: Buried-heterostructure passive feedback laser (BH-PFL)," *IEEE Photon. Technol. Lett.*, vol. 24, no. 5, pp. 362–364, Dec. 13, 2012.
[18] A. Ferrero and U. Pisani, "Two-port network analyzer calibration using an unknown 'thru'," *IEEE Microw. Guided Wave Lett.*, vol. 2, no. 12, pp. 505–507, Dec. 1992.
[19] Y. Rolain, M. Ishteva, E. Van Nechel, and F. Ferranti, "A tensor-based extension for the multi-line TRL calibration," *IEEE Trans. Microw. Theory Techn.*, vol. 64, no. 7, pp. 2121–2128, Jul. 2016.
[20] J. V. Butler, D. K. Rytting, M. F. Iskander, R. D. Pollard, and M. Vanden Bossche, "16-Term error model and calibration procedure for on-wafer network analysis measurements," *IEEE Trans. Microw. Theory Techn.*, vol. 39, no. 12, pp. 2211–2217, Dec. 1991.
[21] C. Lee, *Microwave Photonics*, 2nd ed. Boca Raton, FL, USA: CRC Press, 2013.
[22] M. Oishi, Y. Nishikawa, S. Akiba, J. Hirokawa, and M. Ando, "2-Dimensional beam steering by 2 × 3 photonic antenna using millimeter-wave radio over fiber," in *Proc. IEEE Int. Topical Meeting Microw. Photon. (MWP)*, Oct. 2013, pp. 130–133.

MATEJ KOMANEC received the M.Sc. and Ph.D. degrees in radio electronics from Czech Technical University (CTU) in Prague, Czech Republic, in 2009, and 2014, respectively. Currently, he is a Senior Researcher and an Associate Professor with the Department of Electromagnetic, CTU in Prague. His research interests include microwave photonics, hollow-core optical fibers, fiber-optic sensing, visible light communication, and specialty optical fibers.

LEOS HALMO received the M.Sc. degree from Czech Technical University in Prague, Prague, Czech Republic. He has long-term fiber-optics experience from industry. He is currently a Senior Research and Development Engineer with Argotech a. s., Czech Republic, focusing on photonics packaging.

VIKTOR ADLER received the M.Sc. and Ph.D. degrees from the Faculty of Electrical Engineering, Department of Electromagnetic, Czech Technical University in Prague, Prague, Czech Republic, in 2012 and 2018, respectively. His research interests include microwave interferometric measurements, uncertainties analysis, the design of passive and active microwave circuits, imaging techniques, and radars.

JAN BOHATA received the M.Sc. degree in communications, electronics, and multimedia from the Faculty of Electrical Engineering, Czech Technical University in Prague, Prague, Czech Republic, in 2012, and the Ph.D. degree in radio electronics, in 2018. In 2012, he joined the Wireless and Fiber Optics Group, Department of Electromagnetic, with a primary focus on microwave photonics, fiber, free-space optics networks, and optical communications in harsh environments.

MARTA BOTELLA-CAMPOS received the B.Sc. and M.Sc. degrees in telecommunication technologies, systems and networks from Universitat Politécnica de Valéncia (UPV), Valencia, Spain, in 2019 and 2021, respectively, where she is currently pursuing the Ph.D. degree in telecommunication engineering. In 2021, she joined the Photonic Research Laboratories, UPV. Her research interests include microwave photonics, mmW generation for 5G and beyond, and optical networks.

JAKUB ZVERINA received the M.Eng. degree in microelectronics from Czech Technical University in Prague, Czech Republic, in 2005. He has long-term industrial experience in fiber optics and wafer backend. Currently, he is a Senior Research and Development Engineer with Argotech a. s., Czech Republic, focusing on photonics/microelectronics packaging.

STANISLAV ZVANOVEC received the M.Sc. and Ph.D. degrees from the Faculty of Electrical Engineering, Czech Technical University (CTU) in Prague, in 2002 and 2006, respectively. He is currently a Full Professor, the Deputy Head of the Department of Electromagnetic, and the Head of Wireless and Fiber Optics with CTU. His current research interests include free-space and visible light communications and fiber-optic systems, OLED technologies, and RF over optics.